

LAMA5-inspired adhesive dodecapeptide facilitates efficient dentine regeneration: An *in vitro* and *in vivo* study

Jia Tang  | Haicheng Wang | Di Wu | Zuolin Wang

School and Hospital of Stomatology, Shanghai Engineering Research Center of Tooth Restoration and Regeneration, Tongji University, Shanghai, China

Correspondence

Zuolin Wang, School and Hospital of Stomatology, Shanghai Engineering Research Center of Tooth Restoration and Regeneration, Tongji University, Shanghai 200072, China.

Email: zuolin@tongji.edu.cn

Funding information

National Key Research and Development Program of China, Grant/Award Number: 2018YFE0202200; National Natural Science Foundation in China, Grant/Award Number: 81670962 and 81271110

Abstract

Aim: The primary goal of this study was to investigate the potential effects of A5G81 in inducing reparative dentine (RD) formation both *in vitro* and *in vivo*.

Methodology: Cell adhesion was observed by crystal violet staining and quantified by Sodium Dodecyl Sulphate (SDS) extraction. Cell proliferation was investigated using Cell Counting Kit-8 (CCK-8) assay. Spreading of cytoskeleton was visualized using immunofluorescence staining. Protein expression level of Akt signalling pathway was compared in a human Akt pathway phosphorylation array. Genes that were up or downregulated by A5G81 were identified by RNA sequencing. The mRNA expression of odontoblastic markers was detected by quantitative real-time polymerase chain reaction (qPCR). Moreover, mineralization of human dental pulp cells (hDPCs) was visualized by alizarin red staining and quantified using cetylpyridinium chloride (CPC). A direct pulp-capping model was established in SD rats and the RD formation at 2 weeks after operation was observed using HE staining.

Results: A5G81 (optimal coating concentration: 0.5 mg/mL) promoted hDPCs adhesion and proliferation to a level that was similar to Type I collagen (COL-1). Meanwhile, A5G81 activated Akt signalling pathway, albeit to a lesser extent than COL-1. An inhibition test indicated that A5G81 induced hDPCs adhesion by activating PI3K pathway. A5G81 induced the expression of ECM remodelling genes and odontoblastic genes, which were demonstrated by RNA-seq and qPCR, respectively. In addition, A5G81 efficiently accelerated the mineralization of hDPCs in both immobilized and soluble forms, a property that makes it more applicable in dental clinic. Finally, the pulp-capping study in rats suggested that use of A5G81 could successfully induce the formation of RD within 2 weeks.

Conclusion: Coating of A5G81 to non-tissue culture-treated polystyrene facilitates spreading, proliferation and differentiation of hDPCs, resulting in rapid RD formation in artificially exposed pulp.

KEYWORDS

cell adhesive peptide, dental pulp cells, dentine regeneration, extracellular matrix

INTRODUCTION

Preservation of dental pulp vitality will undoubtedly extend the longevity of a tooth. In deep caries treatment, unexpected pulp exposure may occur during the process of decay removal. To achieve efficient wound healing in exposed pulp, various materials especially calcium hydroxide (CH)-based and calcium silicate (CS)-containing products have been tested in animals and even applied clinically (Peskersoy et al., 2021). However, the hard tissue formation induced herein was primarily due to external calcium release from those materials and their rapid formation of apatite instead of *in situ* human dental pulp cells (hDPCs) differentiation and mineralization (Gandolfi et al., 2015). Therefore, to achieve biological dentine regeneration, it is highly desirable to develop materials that are capable in activating the inherent regenerative potential of dental pulp.

Laminins (LNs) are a major type of cell adhesive extracellular matrix protein in the basement membrane. They contain at least 24 types of proteins composing three sub-chains (α β γ). One of the most broadly and highly expressed of these proteins is laminin alpha 5 (LAMA5), which is indispensable for normal embryonic development (Jones et al., 2020). The important role that LAMA5 plays in dictating the normal development of tooth bud is evident upon its genetic knockout in mice, which results in defective cusp formation and enamel knot development, and interrupted epithelium polarity (Fukumoto et al., 2006). Previously, the potential of iMatrix-511, a fragment derived from LN $\alpha 5\beta 1\gamma 1$ (LN-511), in specifically promoting odontoblast differentiation was demonstrated (Tang & Saito, 2018). Nevertheless, there are problems related to the use of proteins such as high cost and enzymatic degradation. To avoid those shortcomings, peptides are gaining increasing interests over proteins, thanks to their advantages such as ease of synthesis and resistance to enzymatic digestion. Importantly, previous work has already reported the potentiality of a peptide derived from amelogenin in driving dentine regeneration (Peng et al., 2021).

A5G81, a dodecapeptide derived from LG4 domain of LAMA5, has been identified as an adhesive peptide for human dermal fibroblasts (Katagiri et al., 2012). A follow-up study confirmed its high efficacy in closing diabetic dermal ulcers when delivered through a thermo-responsive hydrogel (Zhu et al., 2018). More recently, it was reported that A5G81 could facilitate aged human nucleus pulposus (NP) cells to de-differentiate into a much younger state and could potentially be used to cure disc degeneration (Speer et al., 2021). Those literatures evidenced that A5G81 is highly promising in contributing to wound healing process and tissue regeneration. As

wound healing also occurred shortly after pulp capping, we speculated that A5G81 might play positive roles in enhancing DPCs differentiation and reparative dentine (RD) formation. Therefore, the primary goal of our current study was to investigate the *in vitro* effects of A5G81 in hDPCs and *in vivo* effects of A5G81 in direct pulp capping.

MATERIALS AND METHODS

PRILE and PRIASE guidelines

The manuscript has been written according to the Preferred Reporting Items for Laboratory studies in Endodontology (PRILE) 2021 guidelines (Nagendrababu, Murray, et al., 2021) and the Preferred Reporting Items for Animal studies in Endodontology (PRIASE) 2021 guidelines (Nagendrababu, Kishen, et al., 2021) to depict the main steps involved in conducting the current *in vitro* and *in vivo* experiment (Figures 1 and 2).

Peptides and reagents

Mouse A5G81 (LG4 domain of LAMA5, amino acid sequence: Ala-Gly-Gln-Trp-His-Arg-Val-Ser-Val-Arg-Trp-Gly, AGQWHRVSVRWG) (Figure S1) was custom synthesized by ChinaPeptides via the 9-fluorenylmethoxycarbonyl-based solid phase method. All peptides used in this study had a purity over 95%, as determined by high-performance liquid chromatography (HPLC) and mass spectrometry (MS) analysis (Figure S2).

All reagents were obtained commercially. Dulbecco's Modified Eagle Medium (DMEM) (D6429, Sigma); Fetal Bovine Serum (FBS; F8318, Sigma); antibiotics (1%, 100 U/mL penicillin, 100 μ g/mL streptomycin, 250 ng/mL amphotericin B, Genom Technology); collagenase type I (Yeason); trypsin (Gibco); crystal violet staining solution (E607309, Sangon Biotech); Sodium dodecyl sulphate (SDS, A600485-0500, BBI Life Sciences); water-soluble dexamethasone (Dex, D2915, Sigma); beta-sodium glycerophosphate (β -GP) (G9422, Sigma); ascorbic acid (AA, A4544, Sigma); Alizarin Red S powder (ARS powder, E126BA0007, Sangon Biotech); Neutral buffered formalin (10%, KA1418, Kingmorn); FITC-labeled phalloidin (Yeason); Fluoromount-G[®] (CAT NO. 0100-01, Southern Biotech); cetylpyridinium chloride, monohydrate (CPC, OLD# CD0106-100g, BBI Life Sciences); CCK-8 assay kit (Yeason); Human/Mouse Akt Pathway Phosphorylation Array C1 (AAH-AKT-1-4, RayBiotech); TRIzol reagent (Invitrogen); PrimerScript[™] RT Master

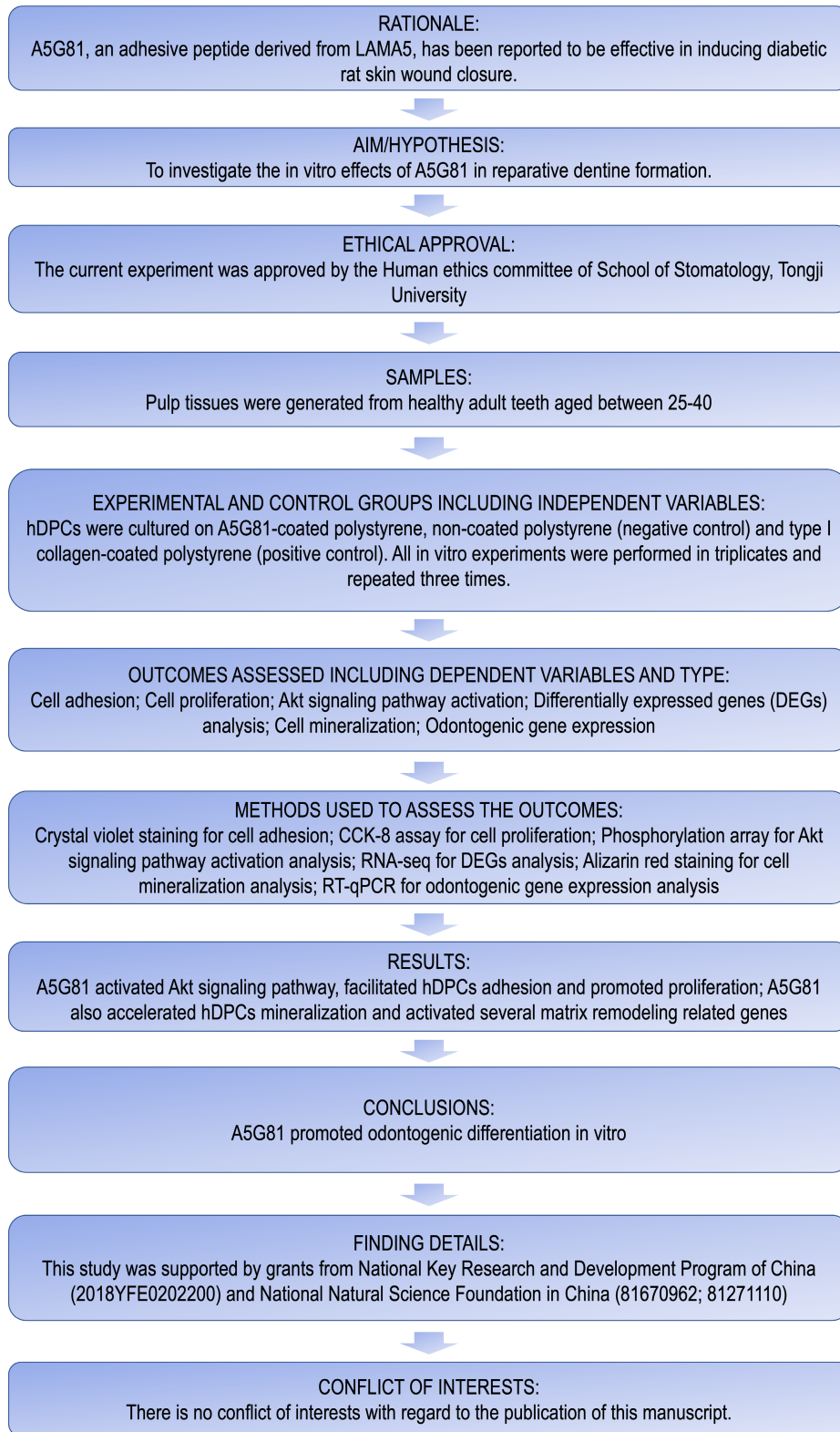


FIGURE 1 PRILE 2021 flowchart illustrating the steps in conducting the current research (*In vitro*).

Mix (Perfect Real Time) (RR036A, TAKARA); Hieff qPCR SYBR Green Master Mix (No Rox, 11201, Yeason); Haematoxylin and eosin (HE) staining solution (Prod#WH2144, WELLBI).

Polystyrene coating

Prior to cell seeding, the non-tissue culture polystyrene plates were pre-coated with A5G81 or COL-1 solution

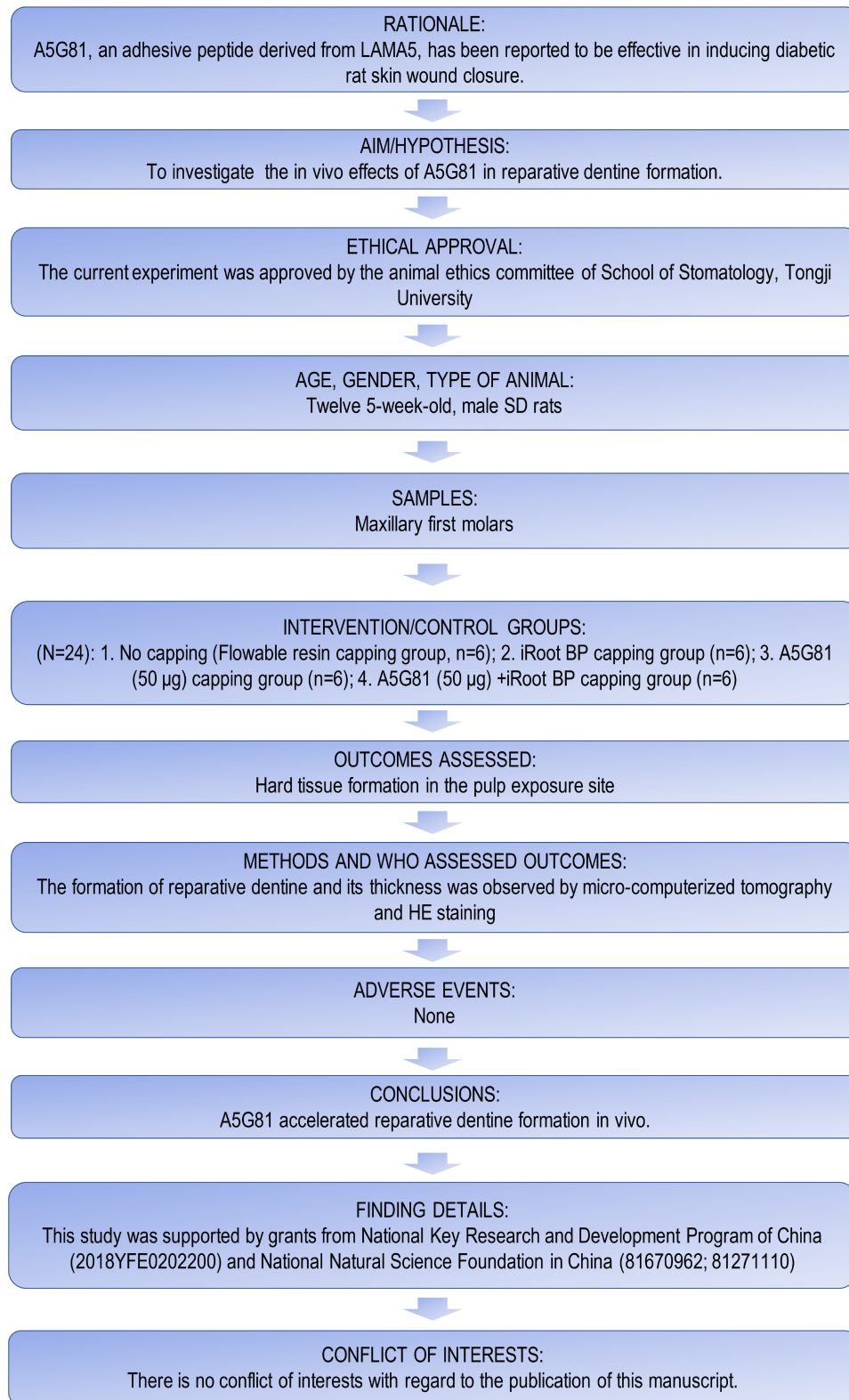


FIGURE 2 PRIASE 2021 flowchart illustrating the steps in conducting the current research (*In vivo*).

diluted by ultra-pure water. Briefly, the A5G81 powder (1 mg/vial) was dissolved in ultra-pure water to make the stock concentration: 1 mg/mL. Various concentrations of A5G81 ranges from 0.0001 to 0.5 mg/mL were prepared

by serial dilution from the stock solution. Similarly, the COL-1 stock solution was diluted by 100 times in ultra-pure water to make the working concentration: 30 µg/mL. Three types of non-tissue culture polystyrene plates

(96-well plate, 12-well plate and 6-well plate) were coated by A5G81 and COL-1. The coating volume for each plate type was 100, 300 and 500 μL , respectively. The coating procedure sustained for at least 48 h under 4°C. Afterwards, the coating solution was aspirated and hDPCs were seeded immediately without washing.

Cell culture

Human dental pulp cells (hDPCs) were collected from the third molars of healthy donors. Inclusion criteria: the donors were 25–40 years old, without systemic diseases, infectious history, caries, pulpitis, periapical periodontitis and root resorption. Informed consent was obtained from patients and isolation of pulp tissue was approved by the Institutional Review Board of School of Stomatology, Tongji University (No. 2022-19). For detailed procedure for isolation of hDPCs, please refer to our earlier article (Tang & Wang, 2023). Briefly, hDPCs were cultured in DMEM supplemented with 10% FBS and 1% antibiotics, which was described as the maintenance media (MM). The MM were changed every 3–4 days and hDPCs were detached and passaged using trypsin at 80%–90% confluence. hDPCs were maintained at 37°C in a humidified atmosphere containing 95% air and 5% CO_2 . Cells at passage number 3–6 were used for the current experiment.

Cell attachment and spreading assays

The cell attachment assay using A5G81 and COL-1-coated plates was performed. Briefly, A5G81 solution with different concentrations (0.001, 0.01, 0.03, 0.05, 0.1 and 0.5 mg/mL) was added and incubated under 4°C for at least 48 h. The detached cells were recovered, suspended in FBS-free DMEM, plated at 6×10^4 /mL and incubated for 2 h at 37°C. The attached cells were fixed and stained with 0.2% crystal violet solution. After washing the non-specific attached staining dye, the cells were photographed under microscope and the staining dye was extracted using 1% SDS aqueous solution. The optical density at 570 nm was measured in a plate reader (SYNERGY H1, BioTek). All assays were carried out in triplicate and each experiment was repeated at least three times.

Cell viability assay

The cells were seeded into three A5G81 and COL-1-coated 96-well non-tissue culture-treated polystyrene plates at the concentration of 3×10^4 /mL. After incubation for 2, 3 and

4 days, CCK-8 reagent was added into each well (10 μL /well) and incubated for 2 h. Then the plate was put into a spectrophotometer to detect absorbance values at 450 nm.

Phosphorylation protein array

The protein detection membrane was blocked using blocking buffer and incubated for 30 min at room temperature (RT). Lysed proteins extracted from non-coated, linear A5G81, cyclic A5G81 and COL-1-coated wells were pipetted into each membrane and incubated at 4°C overnight. Afterwards, the membrane was washed using wash buffer I and II for a total of 25 min. In brief, the detection antibody cocktail was added to each membrane and incubated for 2 h at RT. After that, another round of wash step following the antibody incubation removed unspecific bounding. Following the washing step, HRP-Anti-Rabbit IgG was added into each membrane and incubated for 2 h at RT. After washing, the membrane phosphorylation protein spot was visualized by chemiluminescence detection and recorded by a CCD camera (Amersham™ ImageQuant™ 800 Biomolecular Imager, Cytiva). The expression level of each protein stimulated by A5G81 and COL-1 was semi-quantified using Protein Array Analyzer function in ImageJ.

RNA sequencing

Total RNA was isolated from hDPCs of six groups (three groups for non-coated control and another three groups for A5G81-coated plates) using RNAiso Plus (Cat.# 9108, TaKaRa). Reverse transcription and library construction were performed by Shanghai Majorbio Bio-Pharm Biotechnology Co., Ltd. based on recommendations from manufacturer (Illumina). Sequencing libraries were constructed by Illumina TruSeq™ RNA sample preparation Kit and sequenced using 2×150 bp paired-end configuration on Illumina HiSeq X Ten platform. Gene expression level was calculated using transcripts per million (TPM) reads. Differentially expressed genes (DEGs) were screened by DESeq2 with a filter criteria of fold change (F_c) ≥ 2 and q -value < 0.05 . Functional enrichment analysis including Gene ontology (GO) (<https://geneontology.org/>) and Kyoto Encyclopedia of Genes and Genomes (KEGG) (<https://www.kegg.jp>) was conducted to identify which DEGs were significantly enriched in GO terms and metabolic pathways at Bonferroni-corrected p value $\leq .05$ compared with the whole transcriptome background. GO and KEGG enrichment analysis was performed assisted by Goatools (a python library for GO analysis) and KOBAS (KEGG Orthology-Based Annotation System).

Immunofluorescence staining

For immunocytostaining on A5G81 or COL-1-coated plates, the peptides were coated as described above and cells were inoculated into those non-treated or peptide/protein-treated surfaces in serum-free media. The cells were fixed with 10% neutral buffered formalin for 10 min and permeabilized using 0.5% Triton-X-100 for 5 min. The fixed cells were washed with PBS for 30 min and stained using FITC-labelled phalloidin for 30 min at RT. After that, the cells were thoroughly washed and counterstained with DAPI. Finally, the coverslip with cells were mounted into a glass slide blocked with Fluoromount-G®. Photographs were taken in a Nikon Eclipse Ni fluorescence microscope.

Quantitative real-time polymerase chain reaction

Total RNA was isolated using TRIzol reagent. For reverse transcription of mRNA, random-primed cDNA was synthesized from 1 µg of total RNA using a PrimerScript™ RT Master Mix kit. Real-time PCR analysis was performed using a SYBR Green premix kit from Yeason and detected on a LightCycler® 96 platform (Roche). The reaction conditions for real-time PCR analysis are: 1. 95°C, 30 s, 1 cycle; 2. 95°C, 3 s → 60°C, 30 s → 72°C, 30 s, 45 cycles. GAPDH was used as an internal control for the quantification of mRNA expression. Primer sequences are listed in [Table S1](#).

Western blot analysis

The radioimmunoprecipitation assay buffer (RIPA buffer) (P0013B, Beyotime) and inhibitors cocktail (phenylmethylsulfonyl fluoride solution, PMSF solution, ST507, Beyotime; Protease inhibitor cocktail, P1005, Beyotime; Protein phosphatase inhibitor, P1046, Beyotime) were used for protein isolation at 6 days after inoculation (6-well plate, 50 µL lysis buffer/well). The total protein was diluted five times by water and quantified using Pierce™ BCA assay (23225, ThermoFisher Scientific). Electrophoresis (protein loading amount: 10 µg; EPS 300 protein electrophoresis system, Tanom), transferring and blocking (the polyvinylidene difluoride [PVDF] membrane was immersed in 3% bovine serum albumin [BSA] dissolved in tris-buffered saline containing polysorbate 20 [TBST] at RT for 1 h) were performed in sequence. The primary antibodies used for this experiment were antibodies against COL-1 (1/1000 dilution, rabbit polyclonal antibody, ab34710, Abcam), IBSP (1/1000 dilution, rabbit

polyclonal antibody, BA2329, Boster) and the internal control: β-actin (1/2000 dilution, mouse monoclonal antibody, 8H10D10, #3700, Cell Signaling Technology). After incubation in primary antibodies at 4°C overnight, PVDF membrane was treated with respective secondary antibodies (1/1000 dilutions for both anti-rabbit and anti-mouse secondary antibodies) for 1 h. The bands were visualized using Enhanced Chemiluminescent (ECL) detection kit (SQ101, EpiZyme Scientific) and photographed by an Amersham ImageQuant 800 Western Blot imaging system (Cytiva).

Odontoblastic differentiation assay

The odontoblastic media (OM) consisted of DMEM, FBS (10%), β-GP (10 mM), AA (50 µg/mL) and Dex (10 nM). Cells were seeded into A5G81 and COL-1 coated 6-well plate (Non-tissue culture treated, NEST) (6×10^4 /mL) after digestion with trypsin. When the cells reached 80%–90% confluence, OM was added into each well and changed every 3 days. After 17 days of OM induction, mineralization nodules could be observed under microscope. Alizarin red staining and semi-quantitative analysis were performed after 20 days.

Alizarin red staining and quantification analysis

Alizarin Red S powder was dissolved in distilled water to produce alizarin red dye with a concentration of 1% and the pH of 4.1. The cell monolayer was washed with PBS once and fixed with 10% neutral buffered formalin for 20 min, washed with water once. After that, alizarin red dye was added to cover the cell monolayer and incubated for up to 10 min. Following staining step, cells were washed using water for 2 h to completely remove non-specific background staining. Finally, the stained cells were photographed on a negatoscope. For quantification of staining intensity, CPC was added into each well and incubated for 1 h. The transparent CPC turned purple after addition into stained cells. The purple supernatant was transferred into a new 96-well plate and optical density values for each well was detected at 570 nm by a spectrophotometer.

Rat tooth pulp exposure and direct pulp capping

Five-week male SD rats, weighing 200–300 g, were purchased from Shanghai Legen Biotechnology Co., Ltd.

The operation of animals was approved by the Institutional Animal Care and Use Committee of School of Stomatology, Tongji University (No. 2022-DW-01). The rats were anaesthetised with an intraperitoneal (i.p.) injection of pentobarbital sodium (P3761, Sigma) at a dose of 40 mg/kg. Bowl-shaped cavities with diameters at 0.6 mm were prepared on the centre cusp of the right and left maxillary first molars (M1), using BR-48F (tip diameter: 0.6 mm) diamond point with a high-speed handpiece under water spray. The pulps were then exposed using a K-file (#06). Haemostasis was achieved by wiping the cavity with a sterile gauze. The cavity was gently air dried. For each experimental group, the capping materials were applied as follows: no capping group (NC group, $n=6$); iRoot® BP⁺ plus group (BP group, $n=6$); A5G81 group (A group, $n=6$); iRoot® BP⁺ plus with A5G81 group (BPA group, $n=6$). The adhesives (Single bond universal, 3M ESPE) were used afterwards, left undisturbed for 20 s followed by gentle air blowing and photopolymerized with a light-curing unit for 10 s. Thereafter, flowable light cure composite resin (Revolution formula 2, Kerr Corporation) was applied to the cavity, the surface was gently air blown and photopolymerized with a light-curing unit for 20 s.

Micro-computed tomography evaluation

The SD rats were sacrificed at pre-determined time points, postoperatively. The maxillae with teeth of all groups were isolated and fixed for micro-computed tomography (μ CT) scanning (μ CT 50, SCANCO MEDICAL AG). The scanning parameters were as follows: 70 kV, 200 μ A, 14w, 300-ms exposure time per frame and 7- μ m voxel size.

Tissue preparation and serial sectioning

Two weeks after the operation, the rats were sacrificed using i.p. injection with an overdose of anaesthetic solution mentioned above. The maxillae, along with the experimental teeth, were carefully removed and immersed overnight in 4% PFA at RT for fixation. Excess tissue was trimmed off the specimens, and then they were decalcified with 10% EDTA decalcifying solution (pH 7.4, Wako Pure Chemical Industries Co.) at 37°C for 7 weeks. After decalcification, the resin composite was carefully removed from the cavity and rinsed with running water for 6 h. The tissues were dehydrated in ascending concentration of ethanol solution, dealcoholized by xylene and subsequently embedded in paraffin. Serial sections of 4- μ m-thick slices were cut using a sliding microtome (RM2235; Leica Microsystems) and mounted on

aminopropyl triethoxysilane-coated slides. The sections were deparaffinized with xylene, hydrated in a series of descending grades of ethanol, and then rinsed briefly with tap water and stained by HE for histological observation of RD formation.

Statistical analysis

All the *in vitro* experiments were conducted in triplicate and the results were expressed as the mean \pm standard deviation. Data were subjected to one-way ANOVA and *post hoc* Tukey's multiple comparison tests. Regarding *in vivo* results, the evaluation criteria for RD formation were classified into the following four types: (1) no RD formation (none); (2) RD formation extending from one side to no more than one half of the exposure site (slight); (3) incomplete RD formation extending from one side to more than one half of the exposure site but not completely covering the exposure site (moderate); (4) complete RD formation (intense). Experimental results of *in vivo* study were analysed with a chi-square test to examine the differences between groups. The statistical significance level was set at $p < .05$.

RESULTS

A5G81 enhanced hDPCs adhesion and proliferation, activated Akt signalling pathway

Since cell adhesion is a prerequisite for odontoblast differentiation, we tested the adhesiveness of A5G81 peptide using non-tissue culture-treated polystyrene plates, which was originally used for suspended cell culture. hDPCs adhesion on polystyrene substrates coated by A5G81 diluted in a series of concentration (0.001, 0.01, 0.03, 0.05, 0.1 and 0.5 mg/mL) was assessed by crystal violet staining (Figure 3a). The coating concentration (0.5 mg/mL) was selected for its superior adhesiveness as illustrated by the staining and quantification study (Figure 3b). We next compared the cell adhesiveness of A5G81 (0.5 mg/mL) with COL-1 (30 μ g/mL). The results indicated that this concentration of A5G81 achieved comparable cell adhesiveness as COL-1 (Figure 3c,d). Moreover, result from CCK-8 assay showed that A5G81 promoted hDPCs proliferation better than COL-1 at the initial 2 days (Figure 3e). Except for the cell adhesion and proliferation study, we screened for potential members in Akt signalling pathway that could potentially be activated by A5G81 or COL-1 at 2 days after culture in serum-free media. Akt (Ser-473) was identified by a phosphorylation protein array to be

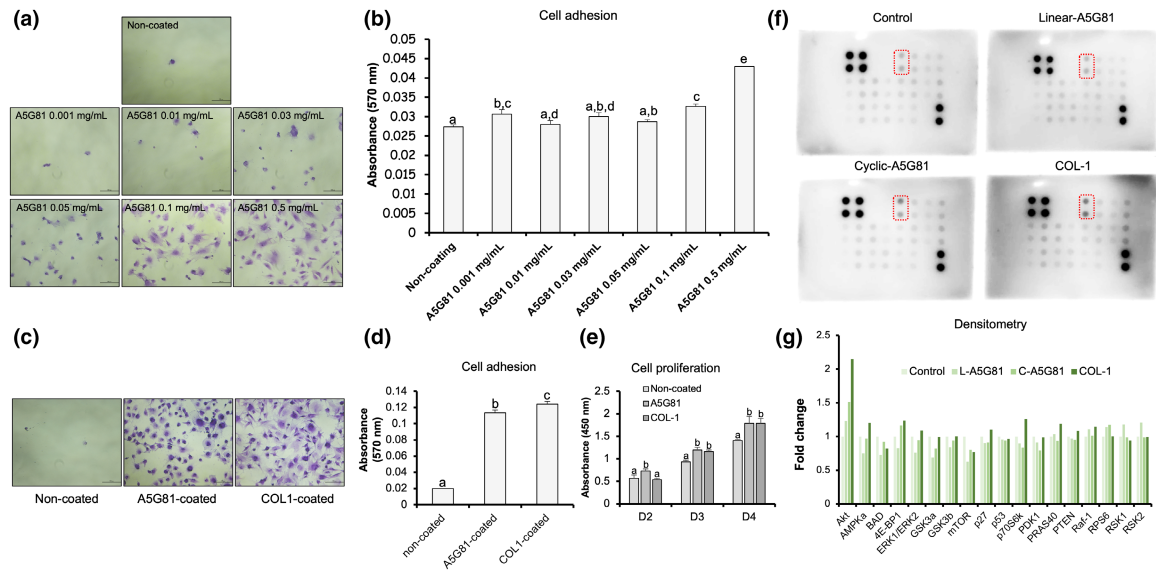


FIGURE 3 A5G81 shows cell adhesiveness, promotes cell proliferation and activates Akt signalling pathway in human dental pulp cells (hDPCs). (a) Photographs of hDPCs adhering to plates coated by a serial concentrations of A5G81; (b) Quantification of cell adhesion levels using SDS reagent in (a), different symbols represent significant differences between groups, $p < .05$; (c) Photographs of hDPCs adhering to A5G81 (0.5 mg/mL) or COL-1-coated plates; (d) Quantification of cell adhesion levels using SDS reagent in (c), different symbols represent significant differences between groups, $p < .05$; (e) Comparison of cell proliferation activity in non-coated group, A5G81-coated group and COL-1 group, different symbols represent significant differences between groups in each specific time points, $p < .05$; Representative arrays (f) and densitometry (g) of Akt signalling pathway in hDPCs cell lysates. Data were normalized over internal positive control (four black points in the upper left side and two black points in the lower right side of the blotting membrane), the red dotted line box in (f) denotes Akt (p-ser 473) or PKB (p-ser 473). L-A5G81: Linear A5G81, C-A5G81: Cyclic A5G81.

activated by both A5G81 (both linear form and cyclic form) and COL-1 (Figure 3f,g) in hDPCs.

A5G81 induced the differentiation and mineralization of hDPCs *in vitro*

RNA-seq analysis was carried out for two groups: hDPCs cultured on linear A5G81-coated (LA5G81) plates and hDPCs cultured on non-coated plates (Control). The correlation analysis of the sequencing samples indicated that replicate samples had high similarity and sound repeatability (Figure S3). The GO annotation analysis revealed that genes related to cell part were significantly influenced by A5G81 (Figure S4). The KEGG annotation and enrichment analysis showed genes involved in sensory system regulation were significantly up- or downregulated by A5G81 (Figures S5 and S6). The detection results were screened according to the aforementioned criteria. Specifically, 148 DEGs were identified by comparing LA5G81 and Control, including 61 upregulated genes and 87 downregulated genes (Figure 4a,b). An interaction network between those genes is shown in Figure 5a. We further screened the DEG data by applying the following criteria: TPM > 0.5; Fc > 2. Five significantly upregulated genes were screened (Figure 5b). Immunofluorescence staining confirmed that PI3K

mediates binding of hDPCs with A5G81 (Figure 6a). To systematically investigate the effects of A5G81 on hDPCs mineralization, both soluble and immobilized forms of A5G81 were applied to observe matrix mineralization. It is shown in Figure 6b–e that both forms of this peptide could effectively promote the mineralization process of hDPCs. To compare the odontoblastic effects between A5G81 and COL-1, qPCR was conducted to assess the mRNA expression of various odontoblastic genes. It is shown that at 1 h after hDPCs inoculation, there were no differences in expression of eight genes in A5G81-coated group (Figure 7a–h left to dotted line), whereas in COL-1-coated group, there were minor elevations in the mRNA expression of *DMP-1* (Figure 7a) and *DSPP* (Figure 7d). When the culture time increased from 1 to 2 h, an inductive potential of A5G81 in eliciting upregulation of odontoblastic genes could clearly be seen in Figure 7b–d,f–h, especially for *COL1A1* and *BSP*, the fold change for both genes was significantly higher in A5G81 group than in control. Although A5G81 promoted the mRNA expression of *DMP-1* at 6 and 19 h, the ascending tendency was terminated at 15 days (Figure 7i–k). In contrary, the mRNA expression of *DMP-1* in COL-1 group was sharply decreased at 15 days (Figure 7k). On the other hand, a constant upregulation of *COL1A1* was observed in A5G81 group (Figure 7l–n). As there was constant upregulation of *COL1A1* mRNA in hDPCs cultured on A5G81 from 2 h to

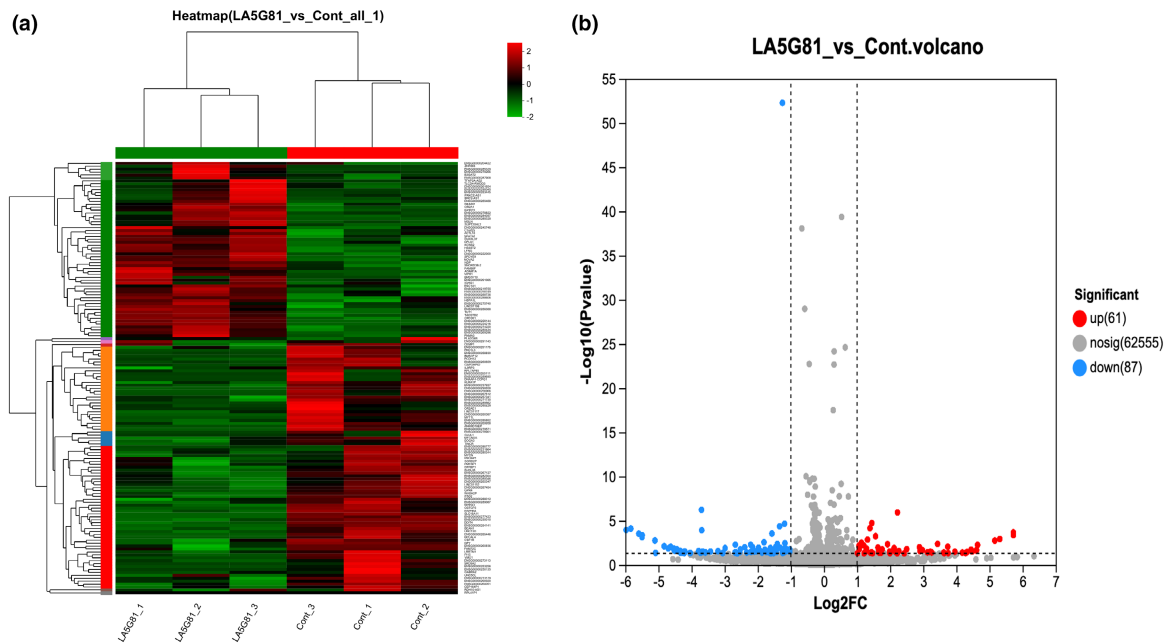


FIGURE 4 A5G81 upregulates 61 genes and downregulates 87 genes at 3 h of human dental pulp cells cultivation. (a) Clustering expression analysis of differentially expressed genes (DEGs). The red colour indicates upregulated genes, while the green colour indicates downregulated genes. (b) Volcano map of DEGs. Red points represent significantly upregulated genes and blue points represent significantly downregulated genes.

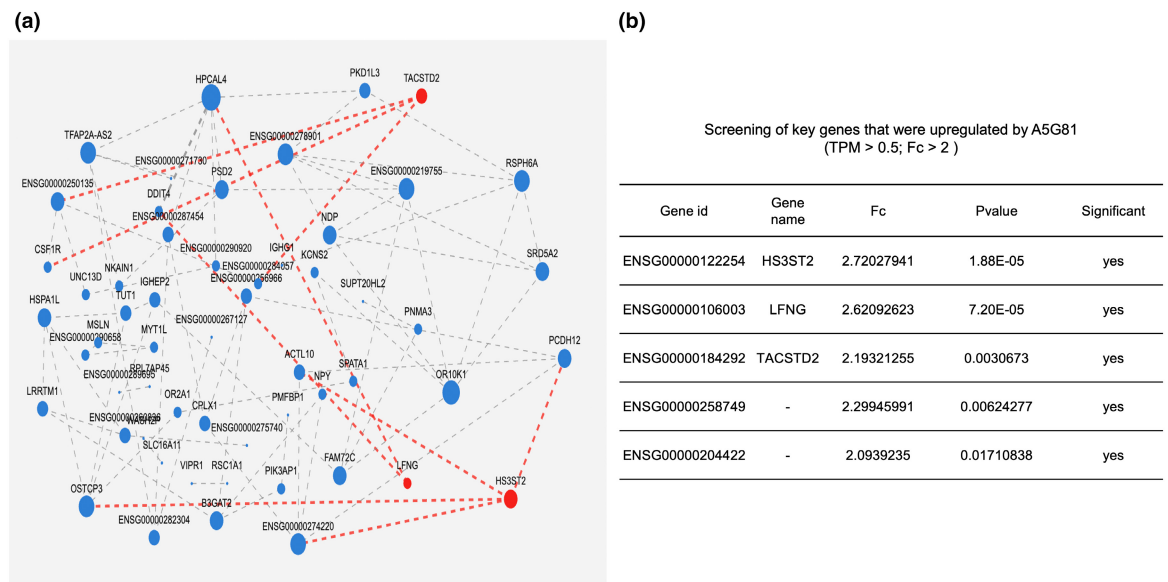


FIGURE 5 A5G81 activates extracellular matrix remodelling genes. (a) Identification of key genes upregulated by A5G81 using RNA-seq data. (b) Gene interaction analysis under GO term cell part (GO: 0044464), red dotted lines represent interaction of three key genes with others.

15 days, we compared the protein expression of COL-1 in different experimental groups, the data revealed that A5G81 promoted COL-1 protein expression in hDPCs compared to noncoated control and COL-1-coated group (Figure 70, upper lane). Meanwhile, the protein expression of BSP was found to be significantly enhanced in A5G81-treated hDPCs

(Figure 70, middle lane). Furthermore, to confirm its superiority in inducing matrix mineralization of hDPCs, cells were cultured on A5G81 for 18 days under osteogenic induction condition and stained by Alizarin red S solution. The result indicated A5G81 promoted hDPCs mineralization better than the control, surprisingly, mineralization in COL-1

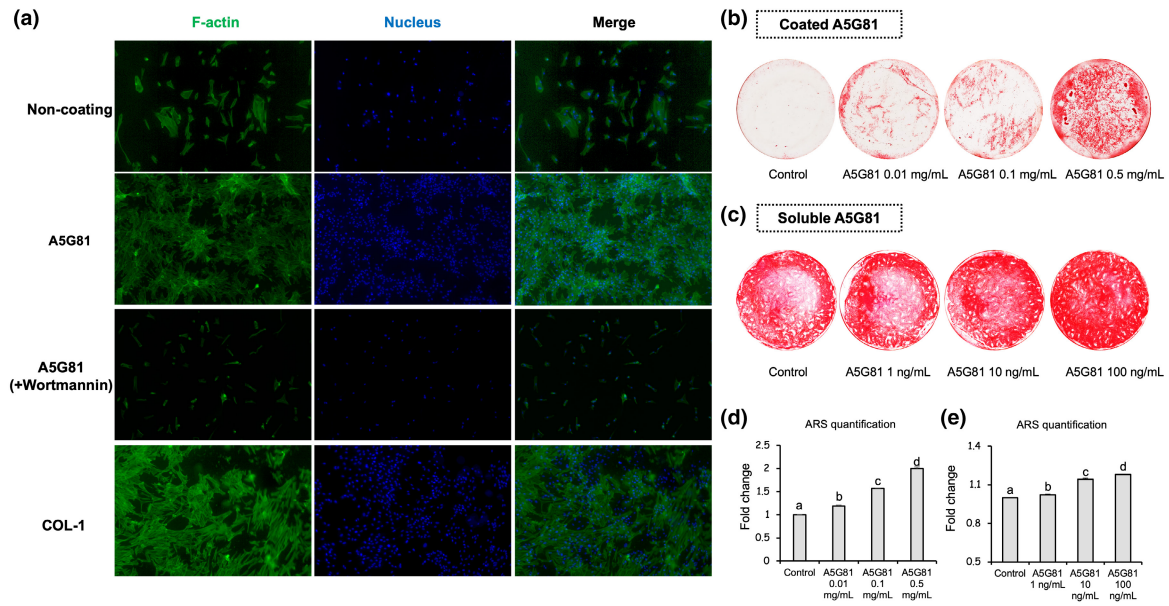


FIGURE 6 A5G81 facilitates human dental pulp cells (hDPCs) adhesion via PI3K and stimulates hDPCs mineralization in both soluble and immobilized form. (a) Immunofluorescence staining of cytoskeleton in hDPCs. Mineralization of hDPCs stimulated by coated A5G81 (0.01, 0.1, 0.5 mg/mL) (b, d) and soluble A5G81 (1, 10, 100 ng/mL) (c, e), different characters represent significant differences between groups, $p < 0.05$, $n = 3$.

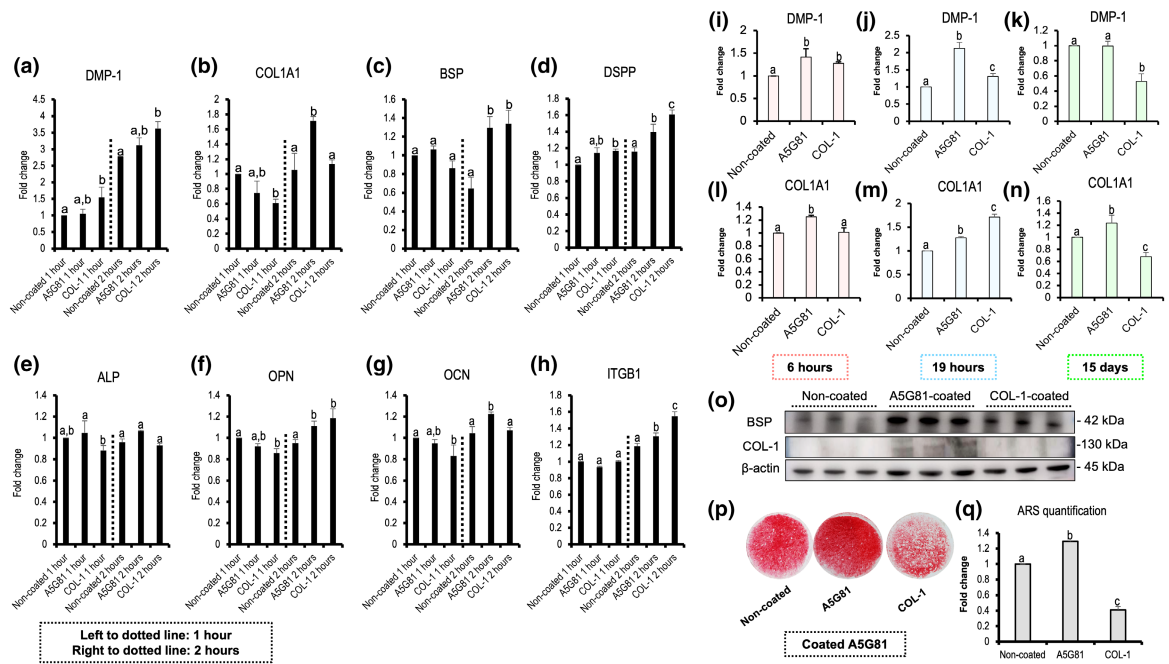


FIGURE 7 A5G81 promotes upregulation of odontoblastic genes and accelerates mineralization better than COL-1. RNA was isolated and subjected to qPCR analysis of *DMP-1* (a), *COL1A1* (b), *BSP* (c), *DSPP* (d), *ALP* (e), *OPN* (f), *OCN* (g) and *ITGB1* (h) at 1- and 2-h exposure. Also, the mRNA expression of *DMP-1* (i: 6 h; j: 19 h; k: 15 days) and *COL1A1* (l: 6 h; m: 19 h; n: 15 days) was shown for both short-term and long-term culture. Western blotting analysis for the protein expression of BSP, COL-1 and β -actin at day six ($n = 3$ for each group) (o). Alizarin red S staining of human dental pulp cells cultured on non-coated or coated substrates is shown in (p) and quantification of staining intensity is shown in (q), the total culture time was 19 days, cells cultured in OM was 18 days. Different symbols represent significant differences between each group in each time point, $p < .05$ by one-way ANOVA Tukey's multiple comparison test, $n = 3$.

group was observed to be reduced as compared to control (Figure 7p,q).

A5G81 accelerated RD formation *in vivo*

The schematic illustration of direct pulp-capping procedure is shown in Figure 8a. After 2 week of the operation, the μ CT and HE staining results indicated that there was no hard tissue barrier formation under the pulp exposure site in NC group (Figure 8b the first group counted from left). In contrast, a continuous layer of newly generated

RD matrix extending from both sides of exposed pulp was observed in iRoot BP⁺ plus group (Figure 8b the second group counted from left). Notably, nearly one third of the specimens in A5G81 group showed intense RD deposition, and the other one third of the same group showed moderate RD formation (Figure 8b,c the third group counted from left). In the BPA (A5G81 + iRoot BP⁺ plus) group (Figure 8b the fourth group counted from left), it was found that similar type of RD was formed as compared to BP group. However, there were fewer specimens with intense RD formation in BPA group than that in BP group. Although iRoot BP⁺ plus was proved to be an

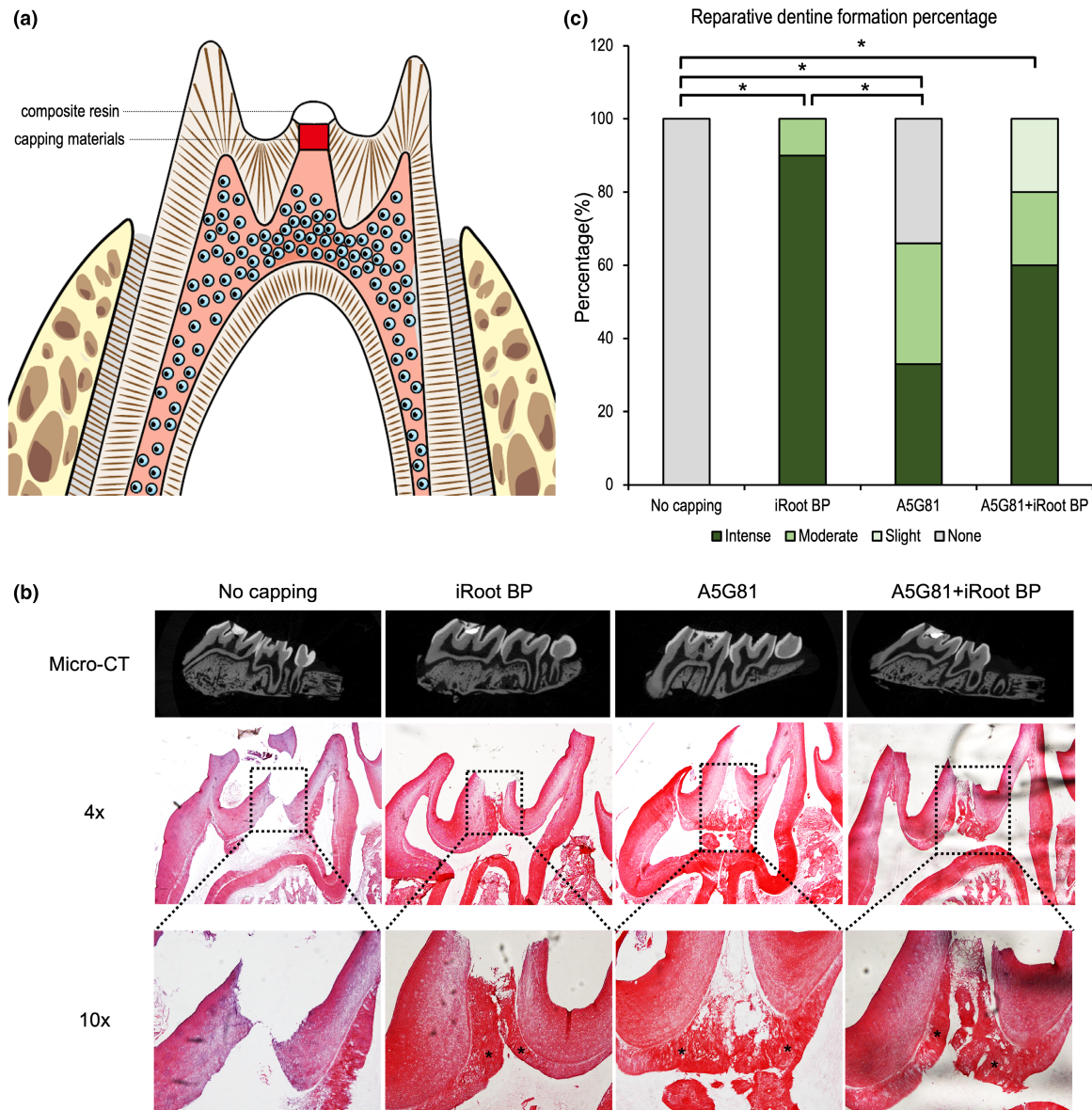


FIGURE 8 μ CT and Histological observation of hard tissue formation at 2 week. (a) Schematic illustration of direct pulp-capping procedure in the central cusp of rat maxillae first molar. (red portion: capping materials; white portion: composite resin). (b) Upper panel: μ CT scanning of rat maxillae with teeth after fixation. Middle panel (4 \times objective) and lower panel (10 \times objective): Histologic features of the sites of pulp exposure based on a 4- μ m-thick section of HE staining at 2 week. * reparative dentine. (c) Statistical analysis of reparative dentine formation rate * $p < .05$.

effective inducer of RD in the current study (Figure 8b), the use of A5G81 alone could also promote the occurrence of RD formation, indicating it might be used as a cofactor for pulp capping.

DISCUSSION

In the past, majority of the research regarding hDPCs has focussed on the effects of various soluble cues, such as growth factors and cytokines (Lan et al., 2022; Vaseenon et al., 2021). Except for those soluble molecules, scaffold-like extracellular matrix (ECM) proteins are another important parameter in dictating cell behaviour. Similar to soluble factors, ECM proteins and their peptide mimetics can bind with cell surface receptors to relay signals intracellularly. More importantly, the nanoscale topography of ECM could profoundly impact the cell proliferation and differentiation, a property that distinguishes them from soluble factors (Su et al., 2022). Based on those observations, research interest is shifting from soluble factors to cell-residing matrix for tissue regeneration. Use of local ECM proteins to recapitulate the microenvironment where cells live may better induce the differentiation of hDPCs towards a desired direction (Fu et al., 2021; Nowwarote et al., 2022). In this preliminary study, we found that a novel recombinant peptide A5G81, derived from basement membrane of tooth germ, promoted hDPCs differentiation and mineralization, accelerated RD formation in rat exposed pulp. The use of A5G81 incurs fewer regulatory hurdles because it triggers the dental pulp's own healing capacity, revealing its broad marketing prospect. By using such a small fragment of LN rather than the entire protein, it can be easily synthesized in the lab, making it more reproducible whilst keeping manufacturing costs low (Gaglione et al., 2019).

Given that a material favouring wound healing should facilitate the spreading, migration and proliferation of surrounding cells into the material, we used cytoplasmic crystal violet staining, fluorescence staining of cytoskeleton to evaluate cell spreading and proliferation of hDPCs. hDPCs seeded in A5G81-coated polystyrene began to spread and interact with the surrounding matrix at 20 min post-seeding (unpublished observation), and by 2 h, cells were fully elongated and displayed fibroblast morphology. In contrast, cells seeded into non-coated polystyrene remained rounded, suggesting minimal interactions with the surface. These findings confirm that the observed cell-matrix interactions are facilitated through specific ligand-receptor interactions between the cells and the tethered A5G81.

For comparative study, we employed a frequently used coating material COL-1 as a positive control in cell

adhesion and proliferation study (Hashimoto et al., 2020). The comparative study of cell proliferation indicated this tiny dodecapeptide manifests equal level of hDPCs adhesiveness as COL-1, a heterotrimer composing over 3000 amino acids (Naomi et al., 2021). The results of an inhibition assay show that anchorage of hDPCs to A5G81 surface was mediated by PI3K, as the number of attached and spread cells was significantly reduced by addition of wortmannin, a specific and potent PI3K inhibitor (Abliz et al., 2015). Moreover, a protein array encompassing most of the members in Akt signalling pathway was conducted. The blotting results indicated that COL-1 and cyclic A5G81 could potentially trigger phosphorylation of Akt (ser-473), an effect that was much stronger than the linear A5G81. The high potentiality of cyclic peptide in eliciting signal transduction was consistent with other literatures (Dai et al., 2022; Zhou et al., 2022). Unfortunately, we cannot observe rapid cell adhesion on cyclic A5G81 as compared to linear A5G81. The possible explanation for this might be due to alteration in conformation of cyclic peptide in the 2D culture plate. Therefore, in the current study, we chose to use linear A5G81 instead of its cyclic counterpart.

To evaluate the progression of odontoblastic differentiation by measuring transcriptional activity, we selected *DMP-1*, *BSP*, *OPN*, *OCN*, *DSPP*, *ALP*, *ITGB-1* and *COL1A1* as differentiation markers of hDPCs. It is clearly shown that A5G81 could trigger the expression of odontoblastic factors at an early stage after cell inoculation. With the increase of time, the difference of expression levels between control and A5G81 group diminished. The phenomenon is reasonable based on the fact that effects imposed by small peptide will be masked by various complete proteins precipitated from culture serum. Since ARS could chelate with calcium cations, Alizarin red S staining is widely used to investigate calcific deposition in cell matrix *in vitro*. Here, we found that both soluble and immobilized forms of A5G81 accelerated the mineralization process of hDPCs. Overall, the pro-proliferation and pro-mineralization properties of A5G81 are expected to provide an optimal microenvironment that facilitates local accumulation of hDPCs and its further differentiation into functional odontoblasts.

To further digging potential key genes that might interact with A5G81 in hDPCs, three genes upregulated by A5G81 were pinpointed: *HS3ST2* (Heparan sulphate glucosamine 3-O-sulfotransferase 2), *LFNG* (Beta-1,3-N-acetylglucosaminyltransferase lunatic fringe) and *TACSTD2* (Tumour-associated calcium signal transducer 2). The former two genes were enzymes that involved in fine-tuning heparan sulphate synthesis (*HS3ST2*) (Teixeira et al., 2020) and modulating NOTCH1 activity (*LFNG*) (Pennarubia et al., 2021). *TACSTD2* is a gene responsible for transducing extracellular calcium signals. It is hence

suggested that A5G81 could potentially influence the ECM remodelling and calcium signal transduction process by upregulated *HS3ST2*, *LFNG* and *TACSTD2*. However, further experiments are warranted to confirm this hypothesis.

The pro-adhesion and pro-mineralization capacity confirmed by *in vitro* experiments prompted us to further explore A5G81's potentiality in forming RD in animals. Indeed, histopathological observation of A5G81-capped rat tooth slice revealed denticle-like RD was successfully induced. Whilst in the BP group, a continuous and much dense layer of RD was formed extending from both mesial and distal sides of pulp exposure, confirming that iRoot BP⁺ plus is a highly efficient pulp-capping agent widely used in the clinic. Although A5G81 alone could induce the formation of RD, the quality of which was inferior to that formed in BP group. Possible explanation could be that iRoot BP⁺ plus is a mixture of tricalcium silicate and other calcium salts, so the formation of a compact layer of RD was primarily due to release of calcium ions (Shi et al., 2016). Regarding A5G81, it is a short peptide harbouring only 12 amino acids, no external calcium was contained in its sequence. Therefore, it is conceivable that the RD induced by A5G81 was thinner and less dense. Therefore, since the pulp tissue was in direct contact with A5G81 in the BPA group, it is also reasonable that the number of intense RD formation specimens was fewer in the BPA group than that in the BP group.

As discussed above, our data uncovered a positive role of A5G81 in stimulating *in vitro* hDPCs differentiation and *in vivo* RD formation, denoting a promising role of A5G81 in vital pulp preservation. Despite the findings, our study has some limitations. First, the physical adsorption was used for peptide immobilization instead of chemical crosslinking. Earlier findings denoted stable immobilization (crosslinking) of peptides on surface could induce much intense activation of intracellular signaling pathways (Hersel et al., 2003). Hence the physical adsorption method we used here may compromise the *in vitro* effects of A5G81. Since stable immobilization of peptides will indeed activate more strongly of intracellular signalling pathways (Hersel et al., 2003). Secondly, the *in vitro* culture condition makes it impossible to monitor cell behaviour on peptide for long term, since various proteins deposited from the serum may mask the effects of peptide gradually. Therefore, development of a stable and controlled release system is necessary for its clinical application in the future.

CONCLUSION

We have identified and characterized a LAMA5-derived peptide with unique receptor-mediated and regenerative properties that are beneficial to the healing process

of exposed pulp. Notably, A5G81 outperformed COL-1 in its ability to induce odontoblastic differentiation and mineralization *in vitro*, and the mechanisms were shown to involve the PI3K/Akt signalling pathway. Furthermore, A5G81 showed a sound potential in inducing rapid formation of RD within 2 weeks. The findings generated from the current work will likely provide a novel target for treatment in regenerative endodontics.

AUTHOR CONTRIBUTIONS

J. Tang conceived the project and designed experiments, performed *in vitro* and *in vivo* experiments, generated and analysed the data, drafted and edited the manuscript; H. Wang and D. Wu contributed to scientific discussions and revised the manuscript. Z. Wang conceived the project, oversaw all the experiments, and critically revised the manuscript. All authors gave final approval and agreed to be accountable for all aspects of this work.

ETHICS STATEMENT

The *in vitro* and *in vivo* experiments were all approved by the local ethics review board in School of Stomatology, Tongji University. For details, see Materials & Methods section (Cell culture; Rat tooth pulp exposure and direct pulp capping).

FUNDING INFORMATION

This study was supported by grants from National Key Research and Development Program of China (2018YFE0202200) and the National Natural Science Foundation of China (81670962 and 81271110).

CONFLICT OF INTEREST STATEMENT

The authors declared there are no conflict of interests with respect to the research, authorship and/or publication of this article.

DATA AVAILABILITY STATEMENT

The data generated from the experiment are available upon proper request to the corresponding author. The raw reads data for the RNA-seq study have already been submitted to Sequence Read Archive (SRA) supported by the NCBI, of which the submission ID and BioProject ID were SUB12534184 and PRJNA923755, respectively. The accession link for raw reads data is: <http://www.ncbi.nlm.nih.gov/bioproject/923755>.

ORCID

Jia Tang  <https://orcid.org/0000-0002-5025-2674>

REFERENCES

- Abliz, A., Deng, W., Sun, R., Guo, W., Zhao, L. & Wang, W. (2015) Wortmannin, PI3K/Akt signaling pathway inhibitor, attenuates

- thyroid injury associated with severe acute pancreatitis in rats. *International Journal of Clinical and Experimental Pathology*, 8(11), 13821–13833.
- Dai, S.A., Hu, Q., Gao, R., Blythe, E.E., Touhara, K.K., Peacock, H. et al. (2022) State-selective modulation of heterotrimeric G α s signaling with macrocyclic peptides. *Cell*, 185(21), 3950–3965.e25.
- Fu, J., Chen, J., Li, W., Yang, X., Yang, J., Quan, H. et al. (2021) Laminin-modified dental pulp extracellular matrix for dental pulp regeneration. *Frontiers in Bioengineering and Biotechnology*, 8, 595096.
- Fukumoto, S., Miner, J.H., Ida, H., Fukumoto, E., Yuasa, K., Miyazaki, H. et al. (2006) Laminin alpha5 is required for dental epithelium growth and polarity and the development of tooth bud and shape. *The Journal of Biological Chemistry*, 281(8), 5008–5016.
- Gaglione, R., Pane, K., Dell'Olmo, E., Cafaro, V., Pizzo, E., Olivieri, G. et al. (2019) Cost-effective production of recombinant peptides in *Escherichia coli*. *New Biotechnology*, 51, 39–48.
- Gandolfi, M.G., Siboni, F., Botero, T., Bossù, M., Riccitiello, F. & Prati, C. (2015) Calcium silicate and calcium hydroxide materials for pulp capping: biointeractivity, porosity, solubility and bioactivity of current formulations. *Journal of Applied Biomaterials & Functional Materials*, 13(1), 43–60.
- Hashimoto, K., Yamashita, K., Enoyoshi, K., Dahan, X., Takeuchi, T., Kori, H. et al. (2020) The effects of coating culture dishes with collagen on fibroblast cell shape and swirling pattern formation. *Journal of Biological Physics*, 46(4), 351–369.
- Hersel, U., Dahmen, C. & Kessler, H. (2003) RGD modified polymers: biomaterials for stimulated cell adhesion and beyond. *Biomaterials*, 24(24), 4385–4415.
- Jones, L.K., Lam, R., McKee, K.K., Aleksandrova, M., Dowling, J., Alexander, S.I. et al. (2020) A mutation affecting laminin alpha 5 polymerisation gives rise to a syndromic developmental disorder. *Development*, 147(21), dev189183.
- Katagiri, F., Ishikawa, M., Yamada, Y., Hozumi, K., Kikkawa, Y. & Nomizu, M. (2012) Screening of integrin-binding peptides from the laminin α 4 and α 5 chain G domain peptide library. *Archives of Biochemistry and Biophysics*, 521(1–2), 32–42.
- Lan, C., Chen, S., Jiang, S., Lei, H., Cai, Z. & Huang, X. (2022) Different expression patterns of inflammatory cytokines induced by lipopolysaccharides from *Escherichia coli* or *Porphyromonas gingivalis* in human dental pulp stem cells. *BMC Oral Health*, 22(1), 121.
- Nagendrababu, V., Kishen, A., Murray, P.E., Nekoofar, M.H., de Figueiredo, J.A.P., Priya, E. et al. (2021) PRIASE 2021 guidelines for reporting animal studies in Endodontology: explanation and elaboration. *International Endodontic Journal*, 54(6), 858–886.
- Nagendrababu, V., Murray, P.E., Ordinola-Zapata, R., Peters, O.A., Rôças, I.N., Siqueira, J.F., Jr. et al. (2021) PRILE 2021 guidelines for reporting laboratory studies in Endodontology: explanation and elaboration. *International Endodontic Journal*, 54(9), 1491–1515.
- Naomi, R., Ridzuan, P.M. & Bahari, H. (2021) Current insights into collagen type I. *Polymers*, 13(16), 2642.
- Nowwarote, N., Petit, S., Ferre, F.C., Dingli, F., Laigle, V., Loew, D. et al. (2022) Extracellular matrix derived from dental pulp stem cells promotes mineralization. *Frontiers in Bioengineering and Biotechnology*, 9, 740712.
- Peng, X., Han, S., Wang, K., Ding, L., Liu, Z. & Zhang, L. (2021) Evaluating the potential of an amelogenin-derived peptide in tertiary dentin formation. *Regenerative Biomaterials*, 8(2), rbab004.
- Pennarubia, F., Nairn, A.V., Takeuchi, M., Moremen, K.W. & Haltiwanger, R.S. (2021) Modulation of the NOTCH1 pathway by LUNATIC FRINGE is dominant over that of MANIC or RADICAL FRINGE. *Molecules*, 26(19), 5942.
- Peskersoy, C., Lukarcinan, J. & Turkun, M. (2021) Efficacy of different calcium silicate materials as pulp-capping agents: randomized clinical trial. *Journal of Dental Sciences*, 16(2), 723–731.
- Shi, S., Bao, Z.F., Liu, Y., Zhang, D.D., Chen, X., Jiang, L.M. et al. (2016) Comparison of in vivo dental pulp responses to capping with iRoot BP Plus and mineral trioxide aggregate. *International Endodontic Journal*, 49(2), 154–160.
- Speer, J.E., Barcellona, M.N., Lu, M.Y., Zha, Z., Jing, L., Gupta, M.C. et al. (2021) Development of a library of laminin-mimetic peptide hydrogels for control of nucleus pulposus cell behaviors. *Journal of Tissue Engineering*, 12, 20417314211021220.
- Su, T., Xu, M., Lu, F. & Chang, Q. (2022) Adipogenesis or osteogenesis: destiny decision made by mechanical properties of biomaterials. *RSC Advances*, 12(38), 24501–24510.
- Tang, J. & Saito, T. (2018) iMatrix-511 stimulates the proliferation and differentiation of MDPC-23 cells into odontoblastlike phenotype. *Journal of Endodontics*, 44(9), 1367–1375.
- Tang, J. & Wang, Z. (2023) Genome wide analysis of dexamethasone stimulated mineralization in human dental pulp cells by RNA sequencing. *The Journal of Gene Medicine*, 25(2), e3466.
- Teixeira, F.C.O.B., Vijaya Kumar, A., Kumar Katakam, S., Cocola, C., Pelucchi, P., Graf, M. et al. (2020) The heparan sulfate sulfotransferases HS2ST1 and HS3ST2 are novel regulators of breast cancer stem-cell properties. *Frontiers in Cell and Development Biology*, 8, 559554.
- Vaseenon, S., Chattipakorn, N. & Chattipakorn, S.C. (2021) Effects of melatonin in wound healing of dental pulp and periodontium: evidence from in vitro, in vivo and clinical studies. *Archives of Oral Biology*, 123, 105037.
- Zhou, Y., Zou, Y., Yang, M., Mei, S., Liu, X., Han, H. et al. (2022) Highly potent, selective, biostable, and cell-permeable cyclic d-peptide for dual-targeting therapy of lung cancer. *Journal of the American Chemical Society*, 144(16), 7117–7128.
- Zhu, Y., Cankova, Z., Iwanaszko, M., Lichtor, S., Mrksich, M. & Ameer, G.A. (2018) Potent laminin-inspired antioxidant regenerative dressing accelerates wound healing in diabetes. *Proceedings of the National Academy of Sciences of the United States of America*, 115(26), 6816–6821.

SUPPORTING INFORMATION

Additional supporting information can be found online in the Supporting Information section at the end of this article.

How to cite this article: Tang, J., Wang, H., Wu, D. & Wang, Z. (2023) LAMA5-inspired adhesive dodecapeptide facilitates efficient dentine regeneration: An *in vitro* and *in vivo* study. *International Endodontic Journal*, 00, 1–14. Available from: <https://doi.org/10.1111/iej.13967>